Fatigue Fract. Engng Mater. Struct. Vol. 9, No. 5, pp. 379–393, 1987
Printed in Great Britain.
8756-758X/87 $3.00 + 0.00

OVERLOAD RETARDATION IN A STRUCTURAL STEEL

C. S. SHIN and N. A. FLECK
University Engineering Department, Trumpington St, Cambridge, CB2 1PZ, U.K.

(*Received in final form* 24 *August* 1986)

Abstract—The mechanisms causing crack growth retardation after an overload were examined for BS4360 50B steel. It was found that plasticity-induced crack closure is the main cause of retardation when the pre-overload growth rate is in the mid-regime of the growth rate versus stress intensity range plot. When the pre-overload growth rate is near threshold it is argued that retardation at the surface of the specimen is primarily due to strain hardening and to the build-up of a favourable residual stress distribution in the material ahead of the crack tip. Supporting evidence for this argument is provided by a preliminary test on 2014A-T4 aluminium alloy. Plasticity-induced crack closure may be a further cause of retardation in the bulk, plane strain regions of the specimens made from BS4360 50B steel and 2014A-T4 aluminium alloy, when the pre-overload growth rate is near threshold.

INTRODUCTION

Many types of engineering component experience occasional overloads during service. Pressure vessels suffer proof loading, rotating machinery are overspeed-tested and aircraft structures encounter occasional strong gusts. Such overloads lead to retardation of a growing fatigue crack and may even result in crack arrest.

Several different mechanisms have been proposed to explain retarded growth of a fatigue crack, following application of an overload. Crack tip blunting by the overload followed by re-initiation of the fatigue crack appears to be the first proposed explanation [1]. Crack tip strain hardening and the generation of a favourable residual stress field ahead of the crack tip have also been suggested [2, 3]; these mechanisms lead to a decrease in the cyclic plastic strain range at the crack tip.

Suresh[4] argues that retardation is enhanced when crack deflections and crack branching accompany an overload: these deviations in crack path lead to a decrease in the crack driving force and to an enhancement of roughness-induced crack closure. Finally, Elber[5] has proposed that retardation is due to the phenomenon of plasticity-induced crack closure. Elber argues that the overload causes large tensile deformations in the material ahead of the crack tip. When the crack advances through this overload plastic zone, an increased residual wake of plastic deformation is left on the crack flanks, causing the crack to shut at high tensile loads.

Among these mechanisms, the crack tip residual stress, crack tip blunting and crack tip strain hardening models predict immediate retardation following the overload. The plasticity-induced and roughness-induced closure models predict delayed retardation. If the overload induces immediate crack branching then immediate retardation is expected;

if the branching occurs after some crack growth from the overload location then delayed retardation is predicted. It should be pointed out that the dominant mechanism causing retardation is a function of the material, the baseline stress intensity range, ΔK_b, the overload ratio and the degree of constraint at the crack tip.

In the present study, the primary cause of retardation is investigated for BS4360 50B structural steel. Attention is focussed on the case where ΔK_b is near the constant amplitude threshold, ΔK_{th}, and the case where ΔK_b is much greater than ΔK_{th}.

GENERAL TEST METHOD

A series of tests was performed as follows:

Test A—An overload was applied to a 3 mm thick pre-cracked specimen made from BS4360 50B steel. The pre-overload growth rate was 10^{-4} mm/cycle, which is far above threshold.

Test B—An overload was applied to 2 mm thick notched specimens made from BS4360 50B steel. The growth rates in these experiments were similar to those in Test A. These tests were performed in order to determine the influence of crack profile on retardation response.

Test C—An overload was given to 25 mm thick pre-cracked specimens made from BS4360 50B steel. The pre-overload growth rate was near threshold at 10^{-6} mm/cycle.

Test D—A similar test to Test C was performed on 6 mm thick 2014A-T4 aluminium alloy, in order to investigate the influence of strain hardening on retardation response.

The chemical composition and mechanical properties of the steel and aluminium alloy are given in Table 1. Compact tension (CT) specimens of width 50 mm and initial notch length 15 mm were used for Tests A, C and D. The starter notch in these specimens consisted of a machined V-shaped slot, and was sharpened using a razor blade. For Test B, single edge notched specimens were made from BS4360 50B steel. In all tests, cracks were grown normal to the rolling direction. The steel specimens were stress relieved at 650°C for 1 h in a muffle furnace, prior to testing. The aluminium alloy was tested in the as-received condition.

Crack length at the surface of the specimens was measured to a resolution of 10 μm with a travelling microscope, and to a resolution of 1 μm by a plastic replication technique [7, 8]. Single-stage plastic replicas were examined under an optical microscope, and in a scanning electron microscope (SEM). Two-stage replicas, giving a positive image of the crack, were made from the single-stage replicas by evaporation with a coating of lead [7]. These replicas were then examined in the SEM. Bulk crack growth was monitored by a DC potential drop method, which could resolve an instantaneous change of crack length of 10 μm. Crack growth rates were calculated from a 7-point quadratic fit to the crack growth data.

Crack closure in the compact tension specimens (Tests A, C and D) was monitored using a back face strain gauge. For the single edge notched specimens in Test B, crack closure was measured by a near-tip clip-on gauge straddling the crack. The sensitivity with which the crack opening stress intensity, K_{op}, could be measured was improved substantially through use of an offset procedure [8, 9]. Low-pass filters with a cut-off frequency of 1 Hz were used to reduce electrical noise. This meant that the test frequency had to be reduced from 10 to 0.05 Hz when taking closure measurements.

Table 1. Compositon and tensile properties of test materials

Material	Composition (%)	Average grain size (μm)
BS4360 50B structural steel	0.14 C 1.27 Mn 0.41 Si 0.0017 P 0.004 S 0.073 Al Remainder Fe	10
2014A-T4 aluminium alloy	4.4 Cu 0.50 Mg 0.80 Mn 0.70 Si Remainder Al	60

Tensile properties parallel to rolling direction

Material	Yield stress (MPa)	Ultimate tensile stress (MPa)	Elongation on a gauge length of 25.4 mm (%)	Monotonic strain hardening index, n	Cyclic strain hardening index*, n'
BS4360 50B structural steel	352	519	36	0.27	0.27
2014A-T4 aluminium alloy	325	446	25	0.17	0.16

*Estimated from Ref. [6].

Crack closure was quantified by the U-value, defined as the fraction of the load cycle for which the crack is open. Thus,

$$U = \frac{K_{max} - K_{op}}{K_{max} - K_{min}} = \frac{\Delta K_{eff}}{\Delta K}$$

where K_{max} and K_{min} are the maximum and minimum stress intensities of the fatigue cycle, $\Delta K = K_{max} - K_{min}$ and $\Delta K_{eff} = K_{max} - K_{op}$.

Test A: Overload test at high ΔK_b

A crack was grown from the starter notch using a constant ΔK of 25 MPa$\sqrt{m}$ and a load ratio, R ($= K_{min}/K_{max}$), of 0.05. The applied loads were shed after crack growth increments of 0.25 mm in order to maintain constant ΔK, using an APPLE-II microcomputer [10]. A specimen thickness of 3 mm was chosen in an attempt to achieve a stress state close to plane stress: the ratio of forward plastic zone size to specimen thickness was of the order of unity. By choosing a sufficiently thin specimen to achieve plane stress conditions it was hoped that there would be little variation in crack growth response along the crack front. This proved to be the case, from a comparison of the surface visual observations and the potential drop measurements, and by examination of the fracture surfaces at the end of the test.

When the crack had grown 5 mm from the starter notch, a single overload was applied. The overload stress intensity, K_{ol}, was 51 MPa$\sqrt{m}$, giving an overload ratio, $(K_{ol} - K_{min})/(K_{max} - K_{min})$, of 2. After applying the overload, the baseline loading of $\Delta K = 25$ MPa$\sqrt{m}$

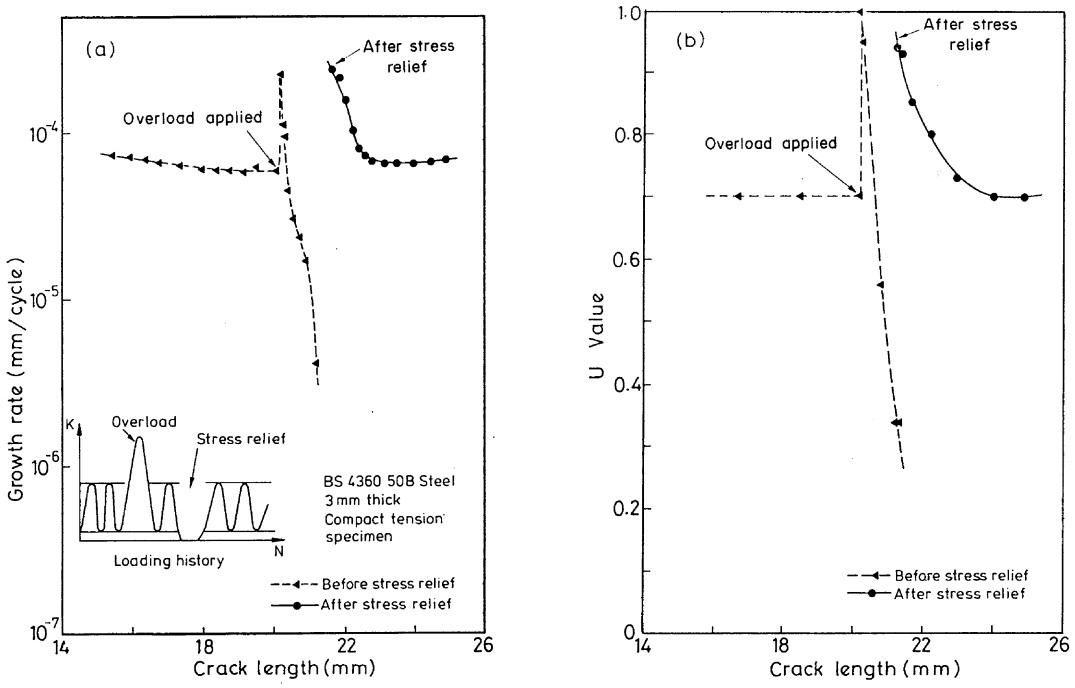

Fig. 1. Effect of a single overload and a subsequent stress relief heat treatment on (a) crack growth rate, and (b) the closure behaviour. Test A, high pre-overload growth rate.

and $R = 0.05$ was resumed and the crack was grown a further 1 mm. To help elucidate the cause of retardation, the specimen was then stress relieved for 1 h at 650°C and the baseline loading was resumed. It was hoped that the stress relief operation would eliminate residual stresses near the crack tip and also remove any plasticity-induced closure of the crack.

Results and discussion on overload test at high ΔK_b

The crack growth rate is given as a function of crack length in Fig. 1(a). Before application of the overload, the crack growth rate was nearly constant at 6×10^{-5} mm/cycle. The replicas shown in Fig. 2 indicate that the overload blunted the crack tip and led to an immediate increase in crack growth rate. The crack then slowed down to about 4×10^{-6} mm/cycle. After stress relief of the specimen, the growth rate increased discontinuously to above the pre-overload value. Finally, the crack attained its pre-overload growth rate.

In order to determine whether crack closure is able to account for this crack propagation behaviour, the crack growth rate, da/dN, is correlated against ΔK_{eff} ($= U\Delta K$) in Fig. 3. The measured U-values given in Fig. 1(b) are used to calculate ΔK_{eff}. It is clear from Fig. 3 that the crack growth data from the present test lie on the same scatter band as that from constant amplitude tests.

The above observations suggest that plasticity-induced crack closure is the dominant cause of retardation following the overload. Other retardation mechanisms play only a minor role, for the following reasons.

Crack tip blunting, strain hardening and the generation of a favourable residual stress field near the crack tip are not dominant since the crack showed delayed retardation rather than immediate retardation after application of the overload. Crack branching is not

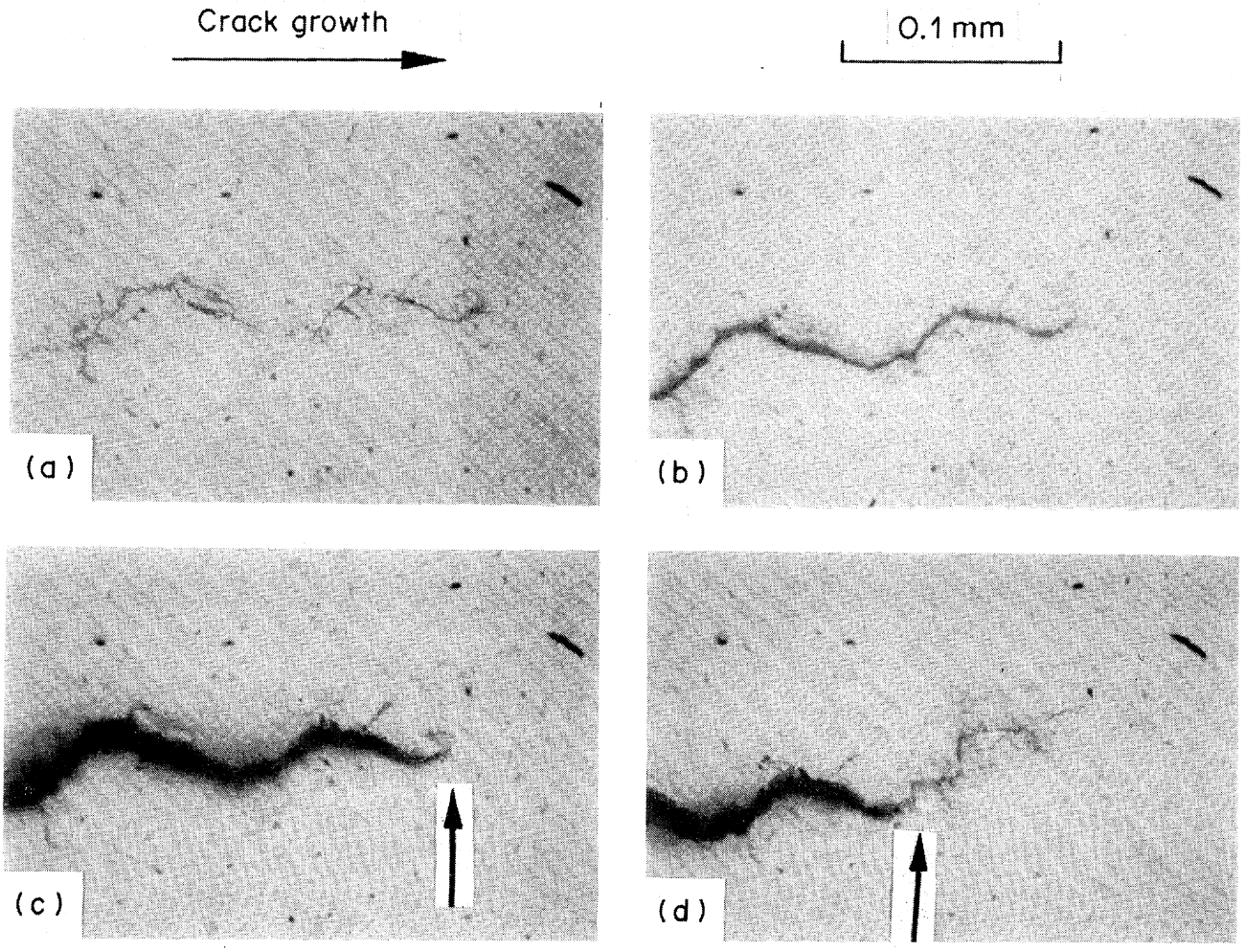

Fig. 2. Plastic replicas from Test A. (a) Immediately before overload (min load). (b) Immediately before overload (max load). (c) Immediately after overload (min load). (d) 300 cycles after overload (min load). The small arrows indicate the position of the crack tip at overload.

important since the crack did not branch following the overload. Roughness-induced crack closure is not the cause of retardation as the overload induced no noticeable change in fracture surface roughness.

Further evidence for the plasticity-induced closure mechanism, and against the mechanisms of roughness-induced closure, crack branching and crack deflections is taken from the stress relief results. A stress relief operation has little effect on fracture surface roughness and crack geometry, yet the crack growth rate, da/dN, increased by nearly 2 orders of magnitude and the U-value increased correspondingly from 0.3 to 0.94 when the specimen was stress relieved. These large increases in da/dN and U are expected if closure is plasticity-induced: a stress relief will relax the compressive residual streses which act across the crack flanks when the crack is closed.

The crack closure transient shown in Fig. 1(b) is now considered in more detail and an explanation is offered for the observed crack propagation response. On application of the overload the crack is blunted such that it remains fully open at K_{min}. The crack growth rate increases by a factor of about 2, reflecting the change in closure value, U, from 0.7 to 1. As the crack advances into the overload plastic zone where residual tensile

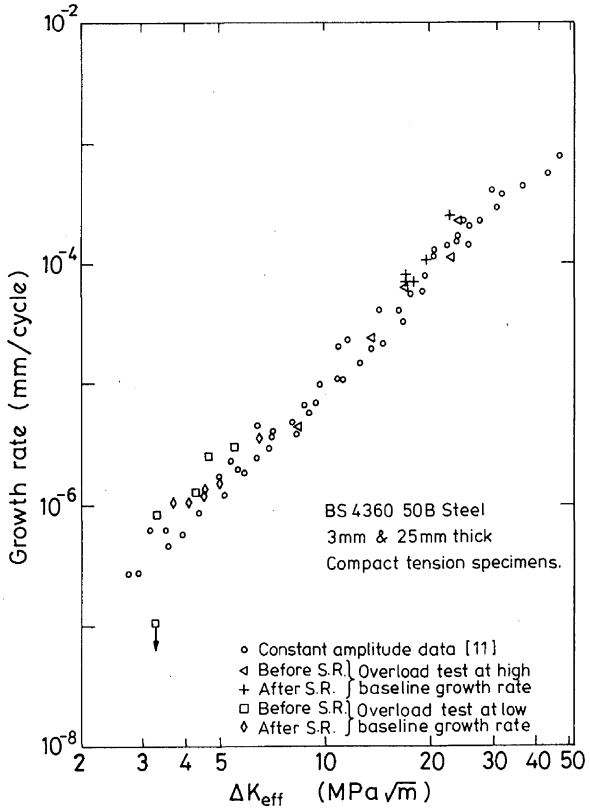

Fig. 3. Assessment of the ability of crack closure to account for retarded growth following an overload in Tests A and C. (S.R.—stress relief.)

deformations have been created by the overload, K_{op} increases. After about 900 cycles following the overload, K_{op} becomes greater than K_{min}, and U drops to less than unity. With further crack growth U decreases to about 0.3, causing a retardation in crack growth rate. Stress relief of the specimen leads to a relaxation of the compressive residual stresses across the crack flanks at zero load, and to a corresponding increase in U. This increase in U causes the crack growth rate to increase by almost 2 orders of magnitude. With subsequent crack growth, the amount of plasticity-induced closure increases again to the steady-state pre-overload value; consequently, the crack decelerates to its pre-overload growth rate.

Test B: Influence of crack profile on retardation response at high ΔK_b

A set of tests was conducted to show that both fatigue pre-cracking prior to the overload and the crack profile at overload have little influence on the retardation response. Single edge notched specimens of thickness 2 mm, length 270 mm and width 140 mm were employed. Semi-elliptical notches with a depth of 35 mm and root radii of 0.4 and 0.7 mm were spark-machined into the side of the specimens. An elastic finite element analysis [12] showed that the stress concentration factor was 22 for the notch of root radius 0.7 mm and 29 for the notch of root radius 0.4 mm. These stress concentration factors are with respect to the nominal stress, σ_{nom}, applied at the ends of the specimen. A cracked specimen was also considered, where the notch was replaced by a saw cut of length 32 mm and a fatigue pre-crack was grown to the same depth as the notch using a stress range, $\Delta\sigma_{nom}$,

of 45 MPa and a load ratio of 0.05. At the end of the pre-cracking operation, the stress intensity range was 22.7 MPa$\sqrt{m}$, and the growth rate was 5.4×10^{-5} mm/cycle.

Each specimen was tested by applying a constant stress range, $\Delta\sigma_{nom}$, of 90 MPa and a load ratio of 0.05, after an initial tensile overload of range 1.5 times that of the baseline loading. Crack growth was monitored with a travelling microscope.

The number of cycles required to initiate a fatigue crack was less than 3000 cycles for the notched specimens, while no re-initiation period was required for the cracked specimen. Figs 4(a) and 4(b) show that, for all three test-pieces, the crack growth responses and the closure responses were identical. Delayed retardation occurred in the notched specimens as well as in the pre-cracked specimen. It is concluded that neither the crack profile at overload nor the fatigue pre-cracking operation prior to application of the overload have a significant influence on retardation behaviour.

The crack growth rate for these specimens is plotted against ΔK in Fig. 4(c) and against ΔK_{eff} in Fig. 4(d). The stress intensity calibration for the notched geometries was calculated by the finite element method [12]. It is clear from Figs 4(c) and 4(d) that crack closure is the main cause of retardation in these test-pieces. Fleck[13] has shown that plasticity-induced crack closure is also the explanation for retarded growth following an overload when plane strain conditions apply and ΔK_b is much greater than ΔK_{th}.

Test C: Overload test at low ΔK_b

Overload tests were also performed on BS4360 50B steel in order to determine the dominant retardation mechanism when ΔK_b is near threshold. Since it was not possible to use a specimen thin enough for plane stress conditions to prevail, a compact tension specimen of thickness 25 mm was employed such that plane strain deformations occurred along nearly the whole crack front (ratio of forward plastic zone size to specimen thickness $\ll 1$). Preliminary tests indicated that the threshold stress intensity range, ΔK_{th}, for BS4360 50B steel is 6.3 ± 0.3 MPa$\sqrt{m}$, at a load ratio, R, of 0.05.

A test was performed by shedding the applied load at a rate $d\Delta K/da = -0.08\Delta K\,mm^{-1}$, using microcomputer control. The initial stess intensity range was 9 MPa$\sqrt{m}$ and the load ratio was fixed at 0.05. When the crack growth rate had decreased to about 10^{-6} mm/cycle, at a ΔK of 6.5 MPa$\sqrt{m}$, a single overload was applied of $K_{ol} = 13.3$ MPa$\sqrt{m}$. Thus, the stress intensity range of the overload cycle was twice that of the baseline cycles. After overload, baseline loading was resumed, using a constant ΔK of 6.5 MPa$\sqrt{m}$.

No sign of crack growth was detected for 7.5×10^5 cycles after the overload. In order to elucidate the cause of retardation, the test was interrupted at this point and the specimen was stress relieved at 650°C for 1 hr. The baseline loading of a constant $\Delta K = 6.5$ MPa$\sqrt{m}$ was resumed; it was found that the crack started to grow again. After a crack growth increment of 2 mm from the overload position, the previous overload test was duplicated: a single overload of $K_{ol} = 13.3$ MPa$\sqrt{m}$ was applied and the specimen was fatigued for 7.5×10^5 cycles with the baseline loading. No sign of growth was detected as before. Finally, the test was stopped and the specimen was sectioned along the mid-plane normal to the thickness direction. One half of the specimen was placed in liquid nitrogen and broken open along the crack plane. The sides of the other half were polished and the crack flanks were examined in the SEM.

Results and discussion on overload test at low ΔK_b

The crack growth rate and closure response associated with application of the first

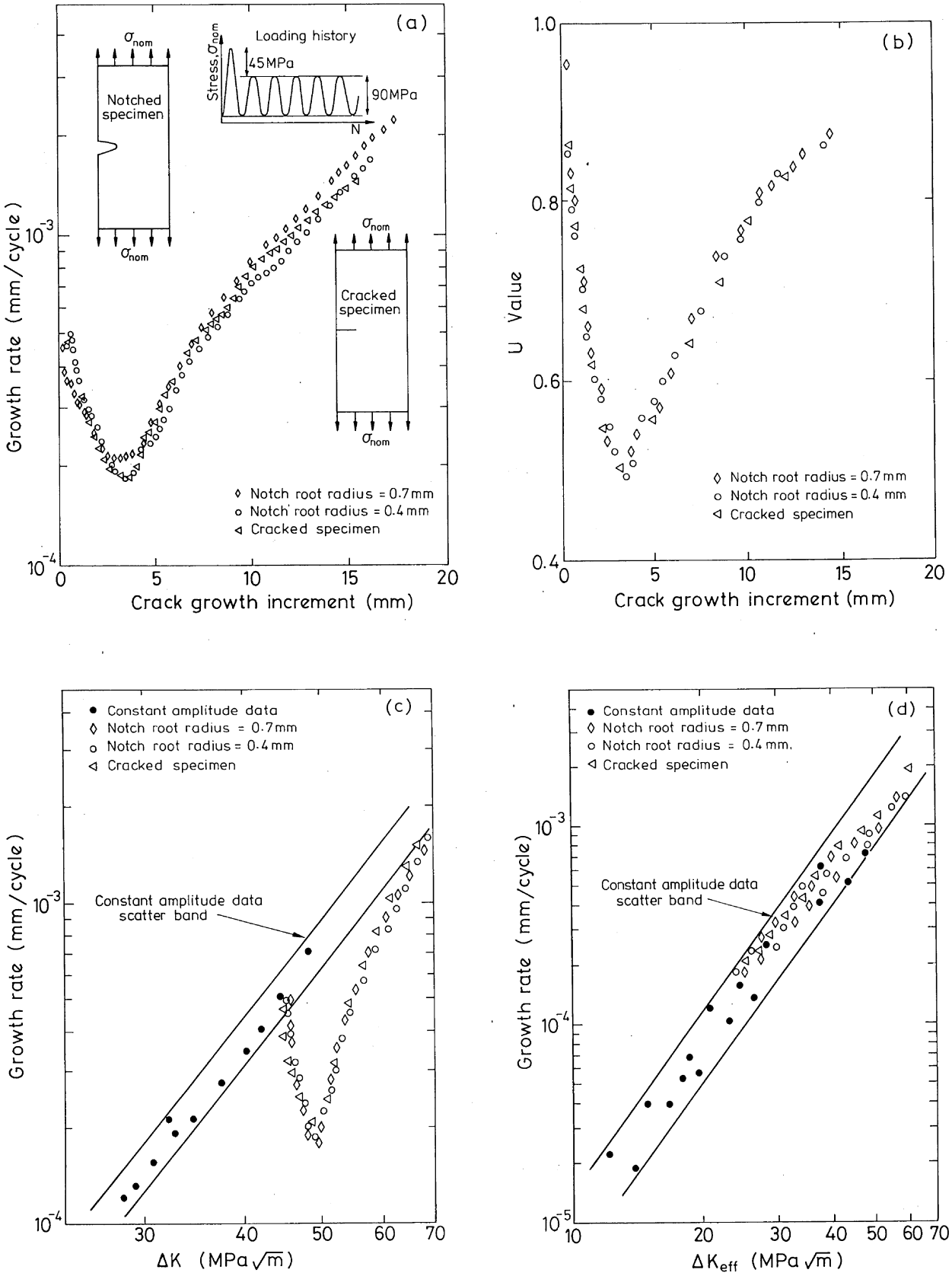

Fig. 4. Results for notched and cracked specimens following a single overload in Test B. (a) Crack growth response. (b) Crack closure response. (c) Crack growth rate vs ΔK. (d) Crack growth rate vs ΔK_{eff}.

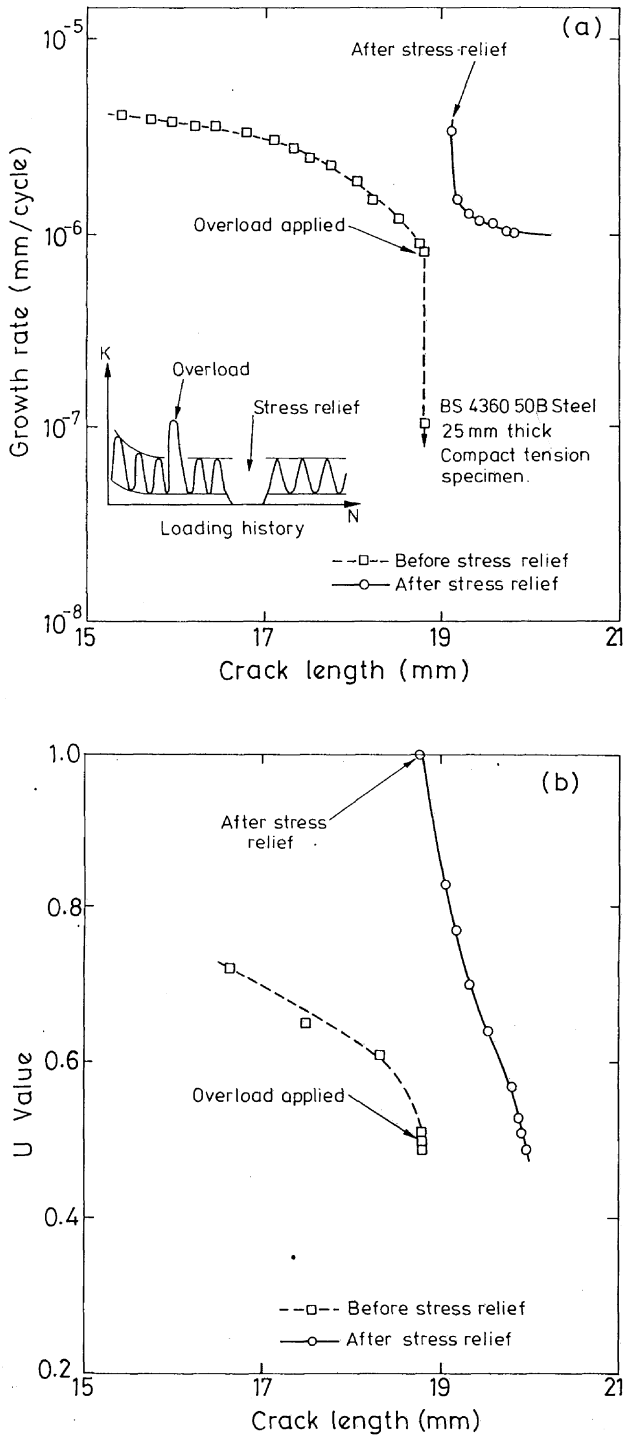

Fig. 5. Effect of a single overload and a subsequent stress relief heat treatment on (a) crack growth rate and (b) the closure behaviour. Test C, pre-overload growth rate near threshold.

overload are given in Figs 5(a) and 5(b), respectively. Prior to application of the overload, the crack growth rate and closure value, U, decreased with decreasing ΔK as the crack grew from the starter notch. After the specimen was overloaded, it was cycled for a further 7.5×10^5 cycles. No crack growth from the overload location was detected on the surface or in the bulk of the test-piece, to within the accuracy of the crack length measurements.

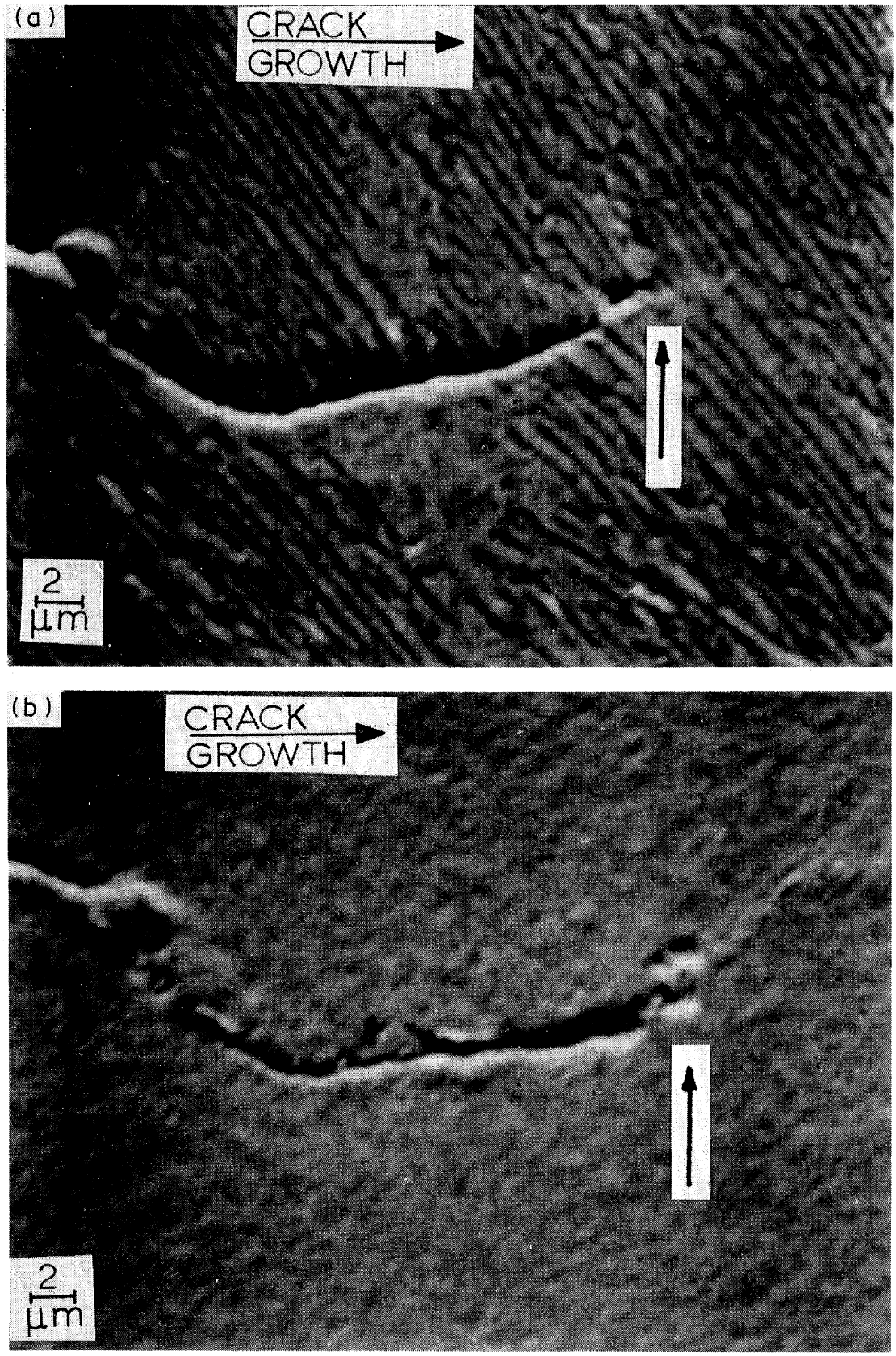

Fig. 6. Replicas of crack profiles on the specimen surface taken at K_{max}, (a) immediately before overload and (b) 7.5×10^5 cycles after the overload. The small arrows indicate the position of the crack tip at overload. Test C, pre-overload growth rate near threshold.

The long term drift of the potential drop method corresponded to 100 μm, thus the crack growth rate throughout the thickness of the specimen was less than 10^{-7} mm/cycle. Double-stage replicas of the crack were taken immediately before and after overload and 7.5×10^5 cycles after overload, in order to measure crack growth at the surface of the test-piece. Observation of these replicas in the SEM indicated a growth rate of less than 10^{-9} mm/cycle (Fig. 6).

In order to determine whether crack growth had occurred after overload, the fracture surface was examined in the region of the second overload, using the SEM. A dark band can be seen on the fracture surface near the end of the region of fatigue crack growth [Fig. 7(a)]. In this band the fracture surface is rougher and faceted [Fig. 7(b)]. It is thought that the start of the band corresponds with the location of the second overload. From the position of the band relative to the region of brittle static fracture it is deduced that the fatigue crack advanced at the centre of the specimen by 80 μm during the 7.5×10^5 cycles following the overload. Similarly, it is deduced that immediate arrest occurred at the surface of the specimen after the overload; this confirms the previous measurement on the replicas that the overload induced immediate crack arrest at the surface. From the fractograph [Fig. 7(a)], the average crack growth increment for the whole crack front following the overload is estimated to be about 60 μm. This was not detected by the DC potential drop technique as it is less than the long term drift.

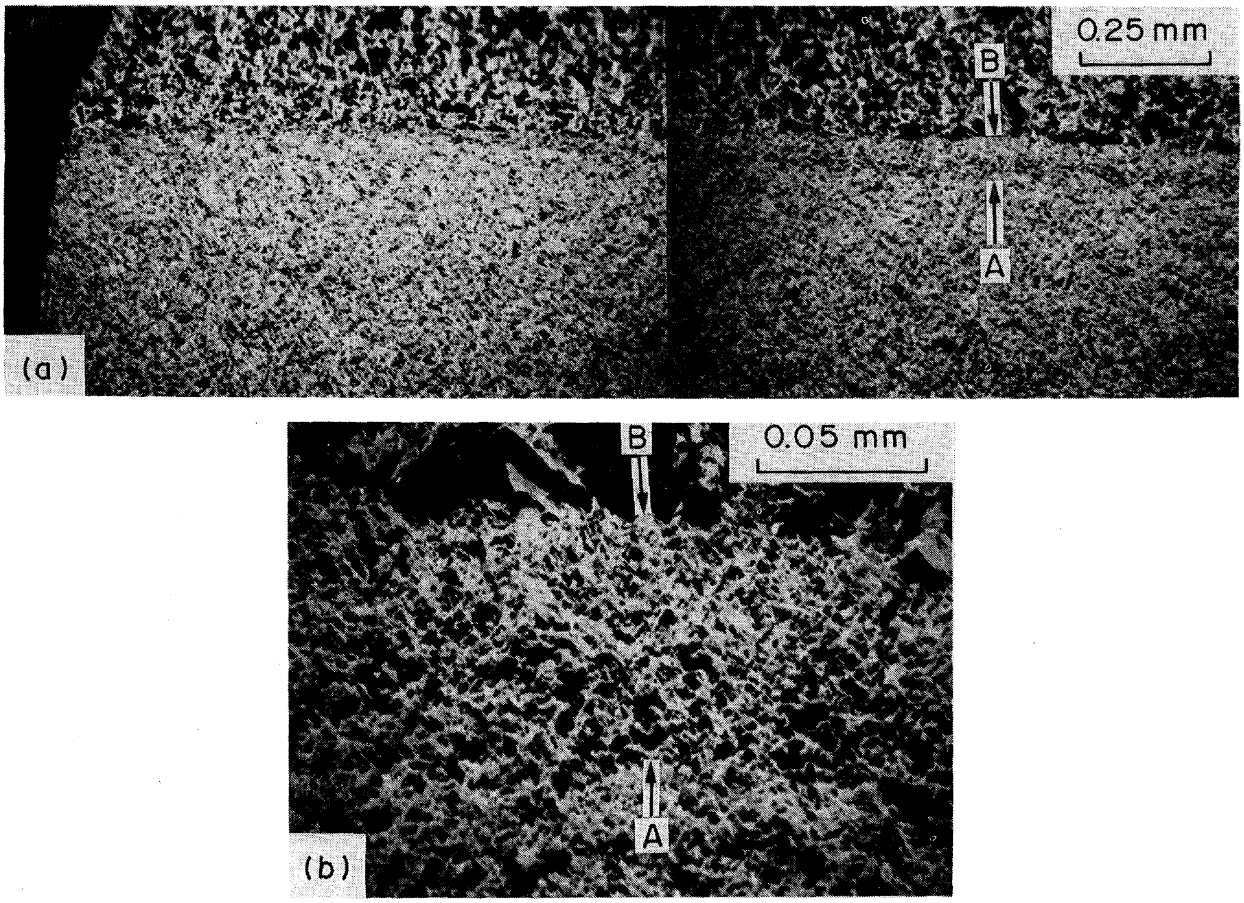

Fig. 7. Fracture surface in Test C (a) due to second overload, a subsequent 7.5×10^5 fatigue cycles and then brittle fracture in liquid nitrogen. Arrow A indicates the overload location, arrow B the start of the brittle fracture region; (b) a close-up of the fracture surface. The arrows refer to the same positions on the fracture surface as in (a).

No significant change in closure load was detected after application of the overload, nor after a further 7.5×10^5 cycles. Thus, the constant amplitude da/dN vs ΔK_{eff} relation is not preserved after application of the overload (see Fig. 3). However, the instrumentation employed was not sensitive enough to detect crack closure over a crack growth increment of the order of 60 μm. If we assume that the crack has advanced 60 μm beyond the overload position before arrest, and that compressive closure stresses equal to the yield stress act over this crack growth increment, then a Dugdale-type calculation predicts an increase in K_{op} of 4.4 MPa$\sqrt{\text{m}}$. Such a rise in K_{op} is sufficient to arrest the crack. Thus, further study is needed to clarify the role of closure in causing crack arrest in the present case.

Crack tip blunting, crack tip branching, or the development of strain hardening and favourable residual stresses at the crack tip may give rise to immediate arrest near the specimen surface. Examination of replicas taken immediately before and immediately after overload showed that the degree of crack tip blunting was minimal. This is consistent with the observation that the overload had no effect on the crack opening load [Fig. 5(b)]. Crack tip branching was also not the cause of retardation for the following reasons.

(1) Examination of replicas taken immediately before overload and 7.5×10^5 cycles later (Fig. 6) indicated that branching was not present at the surface of the specimen. Examination in the SEM of the half of the sectioned specimen not broken open in liquid nitrogen revealed no branching of the crack following the overload.

(2) If crack growth retardation was due to crack branching then it would be expected that the constant amplitude da/dN vs ΔK_{eff} relation would be violated and that a stress relief operation would have no effect on crack growth retardation. It is clear from Figs. 5a and b that the crack growth rate and the closure value U jumped discontinuously to above the pre-overload values after the stress relief treatment. This increase in U is due to relaxation of the compressive stresses acting across the crack flanks by creep, during the heat treatment operation. After stress relief, the constant amplitude da/dN versus ΔK_{eff} relation was preserved (Fig. 3). Thus, crack branching is not the main cause of crack retardation in this material.

The above experimental observations suggest that retardation at the surface may be due to a combination of strain hardening and residual stresses ahead of the crack tip, induced by the overload. These two mechanisms successfully predict immediate arrest following an overload and the elimination of retardation after stress relief of the specimen. Retardation in the mid-thickness region may be due to a combination of the above two mechanisms and plasticity-induced crack closure. At these low growth rates, near threshold closure mechanisms such as oxide-induced crack closure also contribute to the closure phenomenon. They are *not* the cause of retardation, rather they are a *consequence* of a low value of crack driving force; retardation is due to other mechanisms.

The manner in which strain hardening and residual stresses cause retardation may be understood on the basis of a blocked slip band model described by Nakai *et al.* [14]. They argue that the constant amplitude fatigue threshold is attained when the cyclic plastic zone size is equal to a characteristic microstructural unit size, such as the grain size. At threshold, slip is fully reversible in the grains containing the crack tip, and no re-initiation of slip occurs in the neighbouring grains. Now consider application of a tensile overload when ΔK_b is just above threshold. It is argued that an overload increases the dislocation density of grains in the overload plastic zone, leading to strain hardening of this material. On resumption of the baseline cyclic loading cyclic slip ceases in the grains surrounding

the crack tip grain and slip becomes reversible in the crack tip grain. Consequently, the crack arrests. Shakedown to an elastic state of the grains surrounding the crack tip grain is associated with the generation of favourable residual stresses by the overload. At the microscopic level, these residual stresses may be due to the back-stresses on dislocation sources, induced by dislocation pile-ups.

Further evidence that crack arrest at the surface of the specimen is due to a combination of strain hardening and residual stresses was sought by conducting an overload test on 2014A-T4 aluminium alloy (Test D). Whilst the yield stress of this material is comparable with that of BS4360 50B steel, it strain hardens less, see Table 1. Therefore, it is expected that an overload will induce less strain hardening, lower residual stresses and consequently less retardation in the aluminium alloy than in the steel.

Test D: Overload test on 2014A-T4 aluminium alloy at low ΔK_b

A 6 mm thick CT specimen was manufactured from 2014A-T4 aluminium alloy and tested as follows. The stress intensity range was decreased at a fixed load ratio of 0.05 until the crack growth rate was about 10^{-6} mm/cycle. The corresponding stress intensity range, ΔK_b, was 3.8 MPa$\sqrt{\text{m}}$. A single tensile overload of range twice that of the baseline ΔK was then applied, and fatigue loading was recommenced using the same ΔK_b. Crack length was measured using the optical and potential drop techniques described above, and crack closure was measured with a back face strain gauge.

The DC potential drop method indicated that the crack at the centre of the specimen decelerated and arrested after 0.3 mm of growth from the overload location. Similar behaviour was exhibited at the surface of the specimen, where the crack arrested 0.04 mm beyond the overload position.

Examination of single-stage replicas showed that the overload did not induce significant blunting or branching of the crack. Also, no change of crack opening load was observed during the period from application of overload to crack arrest. These closure mesurements are not conclusive since the back face strain gauge is not able to detect crack closure when the closed crack increment is small [11]. More sensitive closure measurements are required in order to determine whether crack growth following the overload is governed by the crack closure phenomenon.

Crack arrest in BS4360 50B steel occurs after a smaller crack growth increment from the overload than in 2014A-T4 aluminium alloy. This is consistent with the argument that an overload induces more strain hardening and greater residual stresses in the steel than in the aluminium alloy.

Overload tests on other materials at low ΔK_b

Suresh[4] and de Castro and Parks[15] conducted overload tests on ASTM 542 low-alloy steel, with ΔK_b near to threshold. They monitored crack length using the DC potential drop method and observed immediate arrest after the overload. In both cases, the load ratio was 0.05, the pre-overload growth rate was near threshold at 10^{-6} mm/cycle and the overload was twice the baseline K_{max}. They employed CT specimens of sufficient thickness to enforce plane strain conditions. de Castro and Parks, using a crack mouth gauge, found that the U-value increased from 0.53 to a constant value of 0.64 upon application of the overload. Suresh reported no closure values.

In the light of the present work, it is thought that immediate arrest occurred at the surface of the specimens of de Castro and Parks, and Suresh. This may be due to a

combination of strain hardening and residual stresses ahead of the crack tip, induced by the overload. Post-overload crack growth below the resolution limit of their potential drop systems may have occurred at the centre of their specimens.

CONCLUSIONS

The following conclusions relate to overload tests performed on BS4360 50B structural steel.

(1) When the baseline stress intensity range, ΔK_b, is much greater than ΔK_{th} and plane stress conditions prevail, retardation is primarily due to plasticity-induced crack closure. The crack profile at overload and the operation of fatigue pre-cracking have little influence on the retardation response, as overloaded cracks and overloaded sharp notches behave in almost identical manners.

(2) When ΔK_b is near threshold and plane strain conditions apply, an overload induces immediate crack arrest at the surface of the specimen but not in the bulk of the specimen. It is thought that the retardation mechanism at the surface of the specimen is a combination of strain hardening and residual stresses ahead of the crack tip. This is substantiated by the observation that immediate crack arrest following an overload does not occur at the surface of a specimen made from 2014A-T4 aluminium alloy, a material which strain hardens much less than BS4360 50B steel. Crack growth retardation in the bulk of the BS4360 50B steel specimen may be due to a combination of plasticity-induced crack closure, strain hardening and residual stresses ahead of the crack tip.

Acknowledgements—One of the authors (CSS) is supported by a Research Fellowship from the Croucher Foundation. Thanks are recorded to Mr D. G. Jones of British Gas Engineering Research Station for provision of the steel. Useful comments from the referees of this paper are also gratefully acknowledged.

REFERENCES

1. Christensen R. H. (1959) *Metal Fatigue*. McGraw–Hill, New York.
2. Jones R. E. (1973) Fatigue crack growth retardation after single-cycle overload in Ti-6Al-4V titanium alloy. *Engng Fract. Mech.* **5**, 585–604.
3. Schijve J. and Broek D. (November 1962) Crack propagation. The results of a test programme based on a gust spectrum with variable amplitude loading. *Aircraft Engineer* **34**, 314.
4. Suresh S. (1983) Micromechanisms of fatigue crack growth retardation following overloads. *Engng Fract. Mech.* **18**(3), 577–593.
5. Elber W. (1971) *Damage Tolerance in Aircraft Structures*, ASTM STP 486, pp. 230–242. American Society for Testing and Materials.
6. Tucker L. E., Landgraf R. W. and Brose W. R. Proposed Technical Report on fatigue properties for the SAE handbook. SAE report 74-279, Automotive Engineering Congress.
7. Brown C. and Smith G. C. (1981) A two stage replication technique for monitoring fatigue crack initiation and early fatigue crack growth. In *Advances in Crack Length Measurement* (Edited by Beevers C. J.), pp. 41–51. EMAS.
8. Fleck N. A. (January 1982) The use of compliance and electrical techniques to characterise fatigue crack closure. Report CUED/C/MATS/TR.89, Cambridge University Engineering Department, U.K.
9. Kikukawa M., Jono M. and Tanaka K. (1976) Fatigue crack closure behaviour at low stress intensity level. *Second Int. Conf. on Mech. Behav. Materials*, Boston, pp. 254–277.
10. Fleck N. A. and Hooley T. (1983) Development of low cost computer control. *Seeco '83—Digital Techniques in Fatigue*, City University, London, March 28–30, pp. 309–316.

11. Fleck N. A. (1984) An investigation of fatigue crack closure. Ph.D. thesis, Cambridge University Engineering Department. Also, Technical Report CUED/C-MATS/TR.104 (May 1984).
12. Shin C. S. and Smith R. A. (1985) Stress intensity factors for cracks emanating from notches. *Proc. Int. Sym. on Microstructure and Mech. Behav.*, October, Xian, China.
13. Fleck N. A. (1984) Influence of stress state on crack growth retardation. *Int. Symp. on Fundamental Questions and Critical Experiments on Fatigue*, Dallas, Texas, October. American Society for Testing and Materials. To be published.
14. Nakai Y., Tanaka K. and Nakanishi T. (1981) The effect of stress ratio and grain size on near-threshold fatigue crack propagation in low-carbon steel. *Engng Fract. Mech.* **15** (3–4), 291–302.
15. de Castro J. T. P. and Parks D. M. (1982) Decrease in closure and delay of fatigue crack growth in plane strain. *Scripta Met.* **16,** 1443–1446.